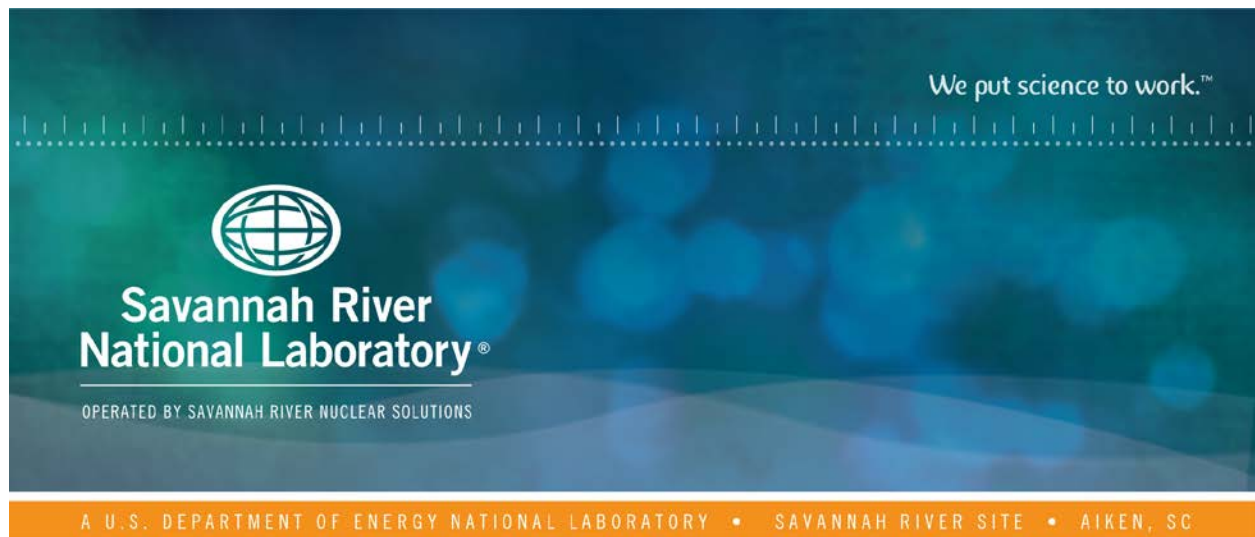**Contract No:**

This document was prepared in conjunction with work accomplished under Contract No. DE-AC09-08SR22470 with the U.S. Department of Energy (DOE) Office of Environmental Management (EM).

Disclaimer:

This work was prepared under an agreement with and funded by the U.S. Government. Neither the U. S. Government or its employees, nor any of its contractors, subcontractors or their employees, makes any express or implied:

1) warranty or assumes any legal liability for the accuracy, completeness, or for the use or results of such use of any information, product, or process disclosed; or
2) representation that such use or results of such use would not infringe privately owned rights; or
3) endorsement or recommendation of any specifically identified commercial product, process, or service.

Any views and opinions of authors expressed in this work do not necessarily state or reflect those of the United States Government, or its contractors, or subcontractors.

2019 Accomplishments - Degradation of mechanical properties in structural metals and welds for GTS reservoirs

Including joint studies with SNL/CA

Timothy M. Krentz
Dale A. Hitchcock
January 2020
SRNL-STI-2020-00002, Revision 0

DISCLAIMER

This work was prepared under an agreement with and funded by the U.S. Government. Neither the U.S. Government or its employees, nor any of its contractors, subcontractors or their employees, makes any express or implied:
1. warranty or assumes any legal liability for the accuracy, completeness, or for the use or results of such use of any information, product, or process disclosed; or
2. representation that such use or results of such use would not infringe privately owned rights; or
3. endorsement or recommendation of any specifically identified commercial product, process, or service.

Any views and opinions of authors expressed in this work do not necessarily state or reflect those of the United States Government, or its contractors, or subcontractors.

Printed in the United States of America

Prepared for
U.S. Department of Energy

2019 Accomplishments - Degradation of mechanical properties in structural metals and welds for GTS reservoirs

Timothy M. Krentz
Dale A. Hitchcock

January 2020

Savannah River
National Laboratory®

OPERATED BY SAVANNAH RIVER NUCLEAR SOLUTIONS

REVIEWS AND APPROVALS

AUTHORS:

_____
Timothy M. Krentz, Energy Materials and Electrochemical Research - SRNL   Date

_____
Dale A. Hitchcock, Energy Materials and Electrochemical Research - SRNL   Date

TECHNICAL REVIEW:

_____
Spencer M. Scott, Energy Materials and Electrochemical Research, Reviewed per E7 2.60   Date

APPROVAL:

_____
Brenda L. Garcia-Diaz, Manager   Date
Energy Materials and Electrochemical Research

_____
Scott McWhorter, Director, Energy Material Science   Date

_____
Scott L. West, Weapons Technology   Date

ACKNOWLEDGEMENTS

EXECUTIVE SUMMARY

This report documents work in 2019 at SRNL in support of the Aging and Lifetimes program. Specimens for fracture toughness testing were prepared in prior years by thermally pre-charging samples, provided by Sandia National Laboratories, of welded types 304L and 21-6-9 stainless steels. These samples were pre-charged in 2017. The fracture toughness of the first aged specimens was measured and compared to historical data. The measurements of the 304L and 21-6-9 weld and particularly HAZ represent some of the first fracture data relevant to modern GTS reservoirs. This work represents an on-going collaboration between SRNL and SNL to understand tritium embrittlement of structural metals in Gas Transfer System reservoirs which informs lifetime assessments.

Continued testing was conducted on ongoing historical studies, including the effects of very long-term aging, and the relative performance of differently forged stockpile relevant 304L and 316L samples.

New samples were pre-charged with tritium and placed in a freezer for an aging study to allow helium to build into the material. The precharged samples consist of smooth and notched tensile samples of 304L stainless steel, as well as tube tensile samples of different thermal treatments supplied by Sandia National Laboratories. Their charging marks the beginning of a new sequence of studies to explore fundamental deformation mechanisms underpinning tritium embrittlement. At predesignated times, samples will be removed from aging and tested to provide data which will help develop an understanding of material degradation with increasing aging time.

Also documented is progress in employing various advanced characterization techniques including high resolution electron microscopy, thermally programed desorption, and small angle x-ray scattering, as well as facilities renovations and equipment procurements in support of sustained tritium impacts on materials program at SRNL.

TABLE OF CONTENTS

LIST OF TABLES

LIST OF FIGURES

LIST OF ABBREVIATIONS

SRNL	Savannah River National Laboratory
SNL (/CA)	Sandia National Laboratories (California campus)
FZ	Fusion Zone (as of a weld)
HAZ	Heat Affected Zone (as of a weld)
appm	Atomic parts per million
TDS	Thermal Desorption Spectroscopy
FIB	Focused Ion Beam

1.0 Introduction

Tritium reservoirs are constructed from forged stainless steels and filled at the Savannah River Site. Austenitic stainless steels are chosen for their good compatibility with hydrogen isotopes, as they are resistant, but not immune, to embrittlement from tritium. In service, hydrogen and its isotopes dissolve into the metal lattice, and, like hydrogen, tritium itself embrittles materials. Additionally, the helium from tritium decay becomes trapped in the microstructure, creating nanoscale bubbles and further reducing toughness. Cracks have been observed in storage vessels after extended service [1-5]. The focus of Savannah River National Laboratory's (SRNL) program on tritium impacts on structural materials is to gather data on the properties of stockpile relevant materials as tritium-decay-helium builds and to inform lifetime assessment and prediction of tritium storage vessels. Further studies continue to improve the understanding of material performance over component lifetimes; as well, new studies are required as novel materials and processes arise.

Four studies are discussed in this report focusing on tritium/helium embrittlement; introducing new investigations or updating ongoing experiments.
1. Examination of the role of microstructure and process-derived strength effects on tensile ductility in 304L after tritium exposure
    o Several new sets of samples have been charged and are currently aging before testing in 2020. These include traditional smooth, as well as notched tensile specimens, and tubes with varying heat treatment and welding histories. All of these new sets of samples are type 304L stainless steel, prepared at SNL/CA for testing by both labs.
2. Examination of weld/HAZ fracture behavior in stockpile-relevant GTS welds after tritium exposure
    o The first round of tests from weld samples developed at Sandia National Laboratories (SNL) are also presented. The full results and optical fractography are included in Appendix A.
3. Long-term tritium aging effects in modern austenitic stainless steel forgings
4. Very long-term tritium aging effects, surpassing 16 years.

Finally, progress towards the application of advanced characterization techniques is briefly noted, along with completed renovations and new equipment procurements.

2.0 Experimental Procedures

2.1 Types 304L and 21-6-9 Stainless Steel Weld Specimens

Samples tested of the types 304L and 21-6-9 stainless steels were fracture mechanics bend bars supplied by SNL/CA. They were machined from weld rings shown in Figure 2-1 to the single edge bend geometry specified in ASTM E1820-18a standard[6]. Typical microstructures are shown in Figure 2-2. Composition of the samples is show in Table 2-1. More details on their fabrication and results with hydrogen pre-charging are found in work by Ronevich et al.[7]
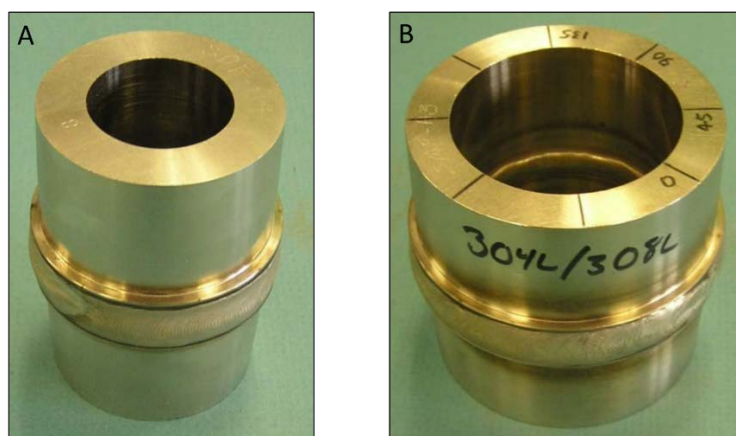
Figure 2-1. Weld Rings: A) 21-6-9 with 308L Filler Metal and B) 304L with 308L Filler Metal
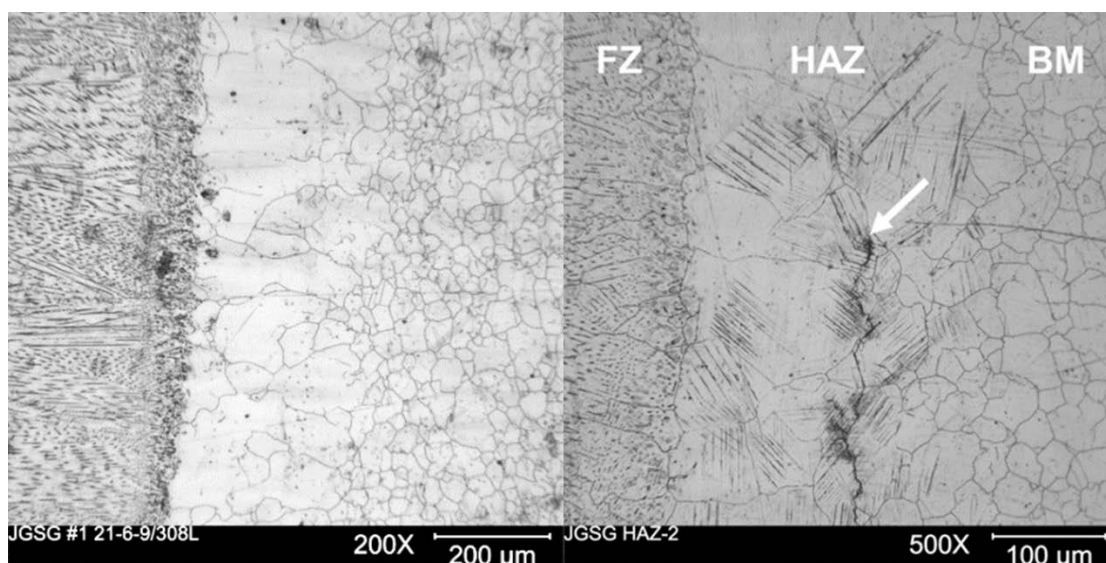
Figure 2-2. (Left) Micrograph of a 21-6-9/308L weld showing the FZ, HAZ and Base Metal (BM). (Right) Micrograph of the same with a precrack terminating in the HAZ, with FZ, HAZ, and BM labeled. Weld Rings and micrographs courtesy SNL/CA, reproduced with permission from [7]

Table 2-1. Composition (wt%) of Base and Filler Metal of SNL/CA Weld and HAZ specimens

Material	Fe	Cr	Ni	Mn	Si	C	N	P	S
304L	Balance	19.38	10.44	1.72	0.57	0.027	0.02	0.021	0.002
21-6-9	Balance	21.06	7.16	9.11	0.53	0.031	0.28	0.015	0.001
308L Filler	Balance	20.5	10.3	1.56	0.5	0.028	0.055	0.006	0.012

Specimens were tritium pre-charged at the Savannah River Tritium Facility in October of 2017. In brief, they were pre-charged under 35 MPa of tritium at 350°C for two weeks. For more details on the conditions of the tritium pre-charging, refer to SRNL-STI-2018-00036.[8]

2.1.1 Fracture testing

Rising displacement fracture toughness tests of the above-described single edge bend specimens were conducted at room temperature in air using a screw-driven testing machine in displacement control at a crosshead speed of 0.002 mm/min while measuring load, crack mouth opening displacement, and crack length via an alternating DC potential drop system. The test setup is shown in Figure 2-3. Similarly, rising displacement tests were conducted on "c" specimens for other ongoing projects. The sample geometry, charging details, and test methods for these are described in prior reports cited in their respective sections below.

Figure 2-3. SRNL's radiological hood (left) and test setup (right) used in testing single edge notched bend bars pre-charged with tritium

2.2 <u>New Sample Charging</u>

Samples prepared by SNL/CA were tritium pre-charged at the Savannah River Tritium Facility in July of 2019. These samples mark the start of a series of test programs laid out in SRNL-STI-2019-00022.[9] Included in this charging were three specimen geometries: 1) tubes with various heat treatment history, 2) smooth tensile, and 3) notched tensile specimens. These samples are all of type 304L stainless steel. Also included in this charging run were type 316L smooth tensile samples prepared by SRNL. A list of the charged specimens follows in Table 2-2. Tube designations denote the heat treatment temperature.

Table 2-2. Samples tritium pre-charged in July 2019

Sample	Material	Specimen ID
SNL Samples		
Type 304L Smooth Tensile	304L	4S1 – 4S36
Type 304L Notched Tensile	304L	4N1 – 4N18
Type 304L As-Received Tubes	304L	AR 10 – AR 19
Type 304L As-Received Tube Welds	304L	No IDs (end notched)
Type 304L 1100F Tubes	304L	Q10 – Q16
Type 304L 1340F Tubes	304L	R10 – R16
Type 304L 1340F Tube Welds	304L	RW10 - RW16
Type 304L 1400F Tubes	304L	S10 – S16
Type 304L 1550F Tubes	304L	T10 – T16
Type 304L 1900F Tubes	304L	U10 – U16
Type 304L 1900F Tube Welds	304L	UW10 – UW16
SRNL Samples		
Type 316L Smooth Tensile	316L	No IDs (bottom bundle)

As in previous charging runs[8, 10], the samples were exposed to nominally 5000 PSIA pressure of tritium at 350°C for two weeks to achieve a homogenous, high concentration of internal tritium. The temperature and pressure data from this charging are shown below in Figure 2-4. The initial spike is a leak check operation, while the sustained plateau is the tritium pre-charging.
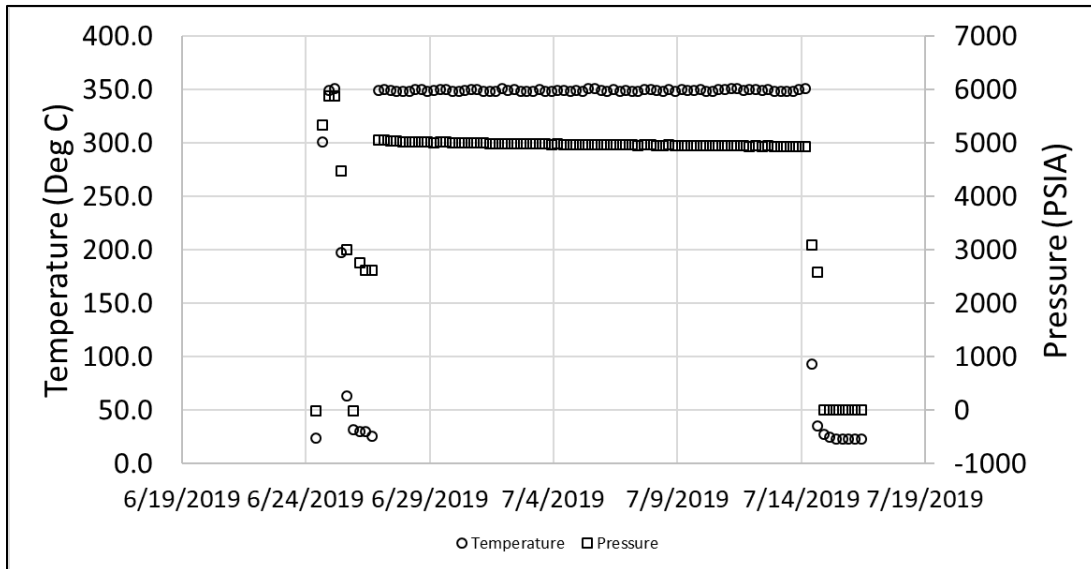
Figure 2-4. Charging history for SNL 2019 samples

After charging, specimens were transferred to SRNL facilities for storage, and were initially held at 0°C for 4 months and were then transferred again when a new -80°C freezer entered into service. These conditions are predicted to yield initial concentrations of 3700 atomic parts per million tritium, based on solubility calculations using data published by San Marchi et al.[11] Temporary storage at 0°C is predicted via diffusion calculations to have a negligible impact on off-gassing, with approximately 1% increase in tritium losses compared to storage at -80°C.

Table 2-3, Table 2-4, and Table 2-5 describe the notional plan for aging and testing these samples. They are grouped as tubes, notched tensile specimens, and smooth tensile specimens respectively and the storage times (aging) to reached desired He-3 levels is shown.

Table 2-3. Tube Tensile Test Matrix

Thermal History	# of Specimens		
	100 ppm He (~6mo)	300 ppm He (1.5 yr)	600 ppm He (3 yr)
As received	2	2	2
As-received welds	2	2	2
1100F	2	2	2
1340F	2	2	2
1340F welds	2	2	2
1400F	2	2	2
1550F	2	2	2
1900F	2	2	2
1900F welds	1	2	2

Table 2-4. Notched Tensile Test Matrix

	# of Specimens		
	100 appm He (6 mo)	300 appm He (1.5 yr)	600 appm He (3 yr)
Failure	2	2	2
Interrupted strain 1	2	2	2
Interrupted strain 2	2	2	2

Table 2-5. Smooth Tensile Test Matrix

	# of Specimens			
	100 appm He (6 mo)	300 appm He (1.5 yr)	600 appm He (3 yr)	1000 appm He (5.6 yr)
Failure	3	3	3	3
5% (true strain)	2	2	2	2
20% (true strain)	2	2	2	2
Failure -5% (true strain)	2	2	2	2

3.0 Results and Discussion

3.1 Weld and Heat-Affected Zone samples

3.1.1 Fracture toughness

The J-integral versus crack length increase (*J* vs. *da*) curves are created from the rising displacement data described above as prescribed in ASTM E1820-18a. These data represent a measure of the resistance to crack growth, or the energy associated with a certain amount of crack extension. J_Q values, the material fracture toughness, are taken as the point where the J vs. da curve crosses an offset of the crack tip blunting

line, constructed from the tensile properties taken from non-charged materials. Three replicates of each sample were tested, and the resulting crack growth resistance curves are shown together in Figure 3-1. As noted above, these samples were charged in October of 2017, and tested in May-June of 2019. Nominal initial tritium contents of 3700 atomic parts per million (appm) in the type 304L stainless steel samples and 6100 appm in the type 21-6-9 stainless steel samples were based on equilibrium calculations from literature properties[11, 12]. At the time of testing, nominal contents of 330 appm helium and 540 appm helium had developed in the 304L and 21-6-9 samples respectively.
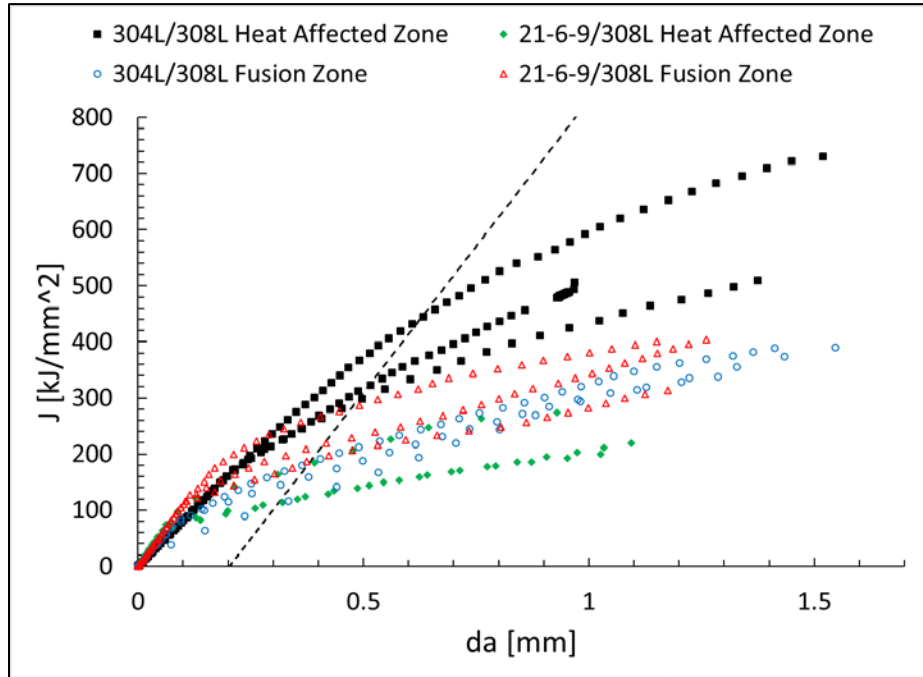
Figure 3-1. Crack Growth Resistance Curves for tritium pre-charged and aged three-point bend specimens of 304L/308L and 21-6-9/308L weld fusion and heat affected zone samples

The dotted line in Figure 3-1 represents the 0.2 mm offset line used in obtaining J_Q values for these samples. Because differing effective flow stresses are used in the analysis for each material, one line with a slope equal to the average flow stress across all samples is used here, simply as a guide for the eye. The values used in analysis are taken from mini-tensile and hardness testing conducted at SNL/CA reported in [13] and from testing at SRNL. These values are additionally shown in Table 3-2.

Values for the fusion zone yield stress and ultimate tensile stress (used in analysis of crack growth data) were measured at SNL/CA for the hydrogen precharged condition. Properties for the HAZ material were calculated from hardness testing also conducted by SNL/CA[13]. The relation between hardness, yield, and ultimate strength is discussed elsewhere[14]. Calculations for yield stress offer good agreement[15] while calculations for ultimate strength are dependent on the particulars of strain hardening, and thus material specific and necessarily at least somewhat empirical[14, 16]. The values used in analysis for all FZ and HAZ samples in this report are compiled in Table 3-1. It may be of interest to conduct further hardness and tensile testing to provide similar values for materials in the tritium precharged and aged condition, as mechanical properties are expected to continue to change with age.

Table 3-1. Compiled mechanical properties for FZ (measured from tensile test) and HAZ (estimated from hardness testing) used in developing crack growth resistance curves

Sample	Yield Strength (MPa)	Ultimate Tensile Strength (MPa)	σ_y(MPa)
304L FZ	338	586	462
21-6-9 FZ	427	676	552
304L HAZ	296	510	407
21-6-9 HAZ	469	717	593

The resulting J_Q values are reported below in Table 3-2, along with averaged J_Q values from corresponding control specimens pre-charged with hydrogen and tested by SNL/CA, as reported in [7, 13]. Note that the hydrogen charging level was approximately twice that of tritium. The full curves for each sample, along with their construction lines and images of fracture surfaces are recorded in Appendix A. The fractography displays both fracture surfaces from each specimen, revealing the notch, side grooves, smooth fatigue pre-crack, and rougher test regions of the fracture. The FZ samples display visible elongated patterns in fracture surface due to the texture in the directionally solidified grains and ferrite compared to HAZ samples. Heat tinting to mark and measure final crack lengths is not feasible due to the potential to evolve unacceptable amounts of tritium, and thus crack lengths are estimates from empirical relations in the ASTM standard[6]. In all but the type 21-6-9 sample HAZ, the percent difference between tritium-precharged and aged samples and samples precharged with approximately twice the hydrogen appm was comparable to or less than the standard deviation specimen to specimen. The type 21-6-9 sample HAZ exhibited a significant decrease in fracture toughness over the hydrogen charged equivalent material. This trend where the embrittlement from moderate helium ingrowth in addition to the remaining tritium roughly compares to the embrittlement from twice the initial hydrogen content agrees with results shown in the past at SRNL[17].

Table 3-2. Tabulated values of J_Q reported for 304L/308L and 21-6-9/308L weld heat affected zones and fusion zones after tritium charging and aging. For comparison J_Q values are shown from specimens precharged in hydrogen and tested at SNL/CA. Note that the concentration of H₂ was slightly more than twice the charging level for T₂, so a direct comparison cannot be made.

304L/308L Heat Affected Zone				
Specimen ID	HAZa-6	HAZa-8	HAZa-9	average	Ave. J_Q with H_2 precharge – SNL/CA
J_Q (kJ/m²)	335	389	547	424	489
21-6-9/308L Heat Affected Zone				
Specimen ID	HAZb-1	HAZb-2	HAZb-3	average	
J_Q (kJ/m²)	110	174	111	132	363
304L/308L Fusion Zone				
Specimen ID	4FZ-1	4FZ-2	4FZ-3	average	
J_Q (kJ/m²)	159	113	192	155	121
21-6-9/308L Fusion Zone				
Specimen ID	9FZ-1	9FZ-2	9FZ-9	average	
J_Q (kJ/m²)	215	278	186	226	196

3.1.2 Fractography

Specimens from each material type have been submitted for fractography. The 304L/308L system HAZ and FZ regions can be seen in Figure 3-2 and Figure 3-3 respectively. The 21-6-9/308L system HAZ and FZ regions can be seen in Figure 3-4 and Figure 3-5 respectively. Obvious qualitative differences can be

seen in both the macro-scale and microscale appearance of the fracture surfaces. The HAZ B material displays evidence of brittle fracture, while the 9FZ material displays both large scale plasticity and prototypical plastic fracture surface features. This agrees well with the average toughness values measured, as the HAZ B material was significantly less tough than the 9FZ. However, in the 304L/308L system, behavior is less straightforward and while fracture surfaces appear more ductile in the 4FZ material than the HAZ A, the HAZ A displays significantly higher fracture toughness in this system.
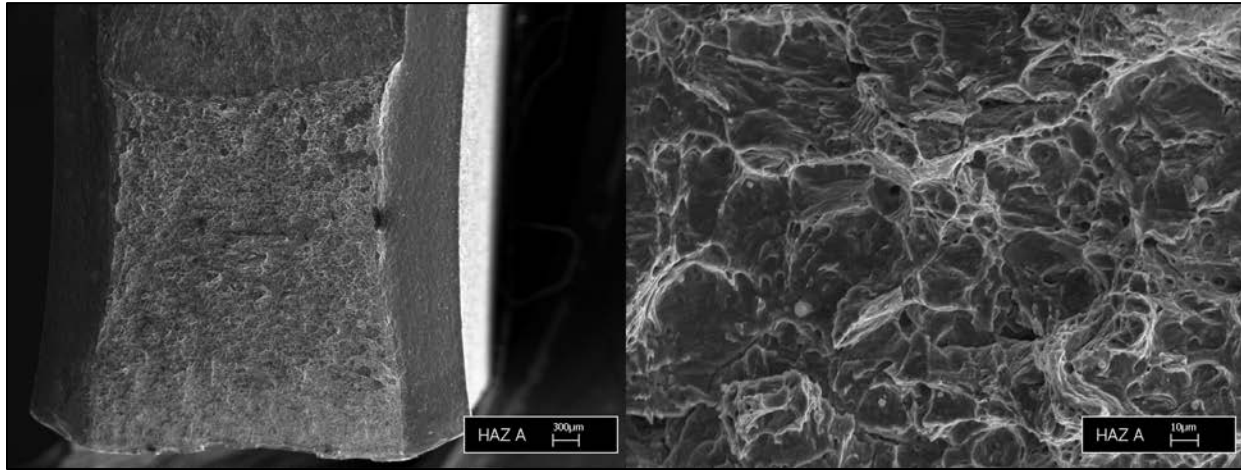
Figure 3-2. HAZ A material prototypical fractography images. Left shows a broad overview of the fracture surface, where the notches are the smooth edges, the fatigue pre-crack is visible as the smooth region at the top, and the crack grown in the test proceeds down the image. Right shows a higher magnification of the test crack region
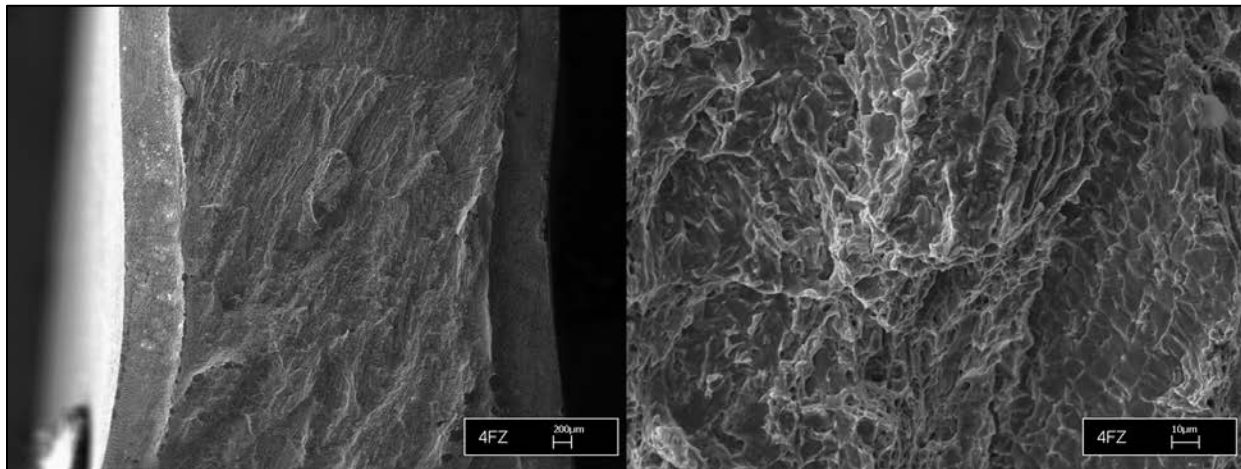
Figure 3-3. 4FZ material prototypical fractography images. Left shows a broad overview of the fracture surface, where the notches are the smooth edges, the fatigue pre-crack is visible as the smooth region at the top, and the crack grown in the test proceeds down the image. Right shows a higher magnification of the test crack region
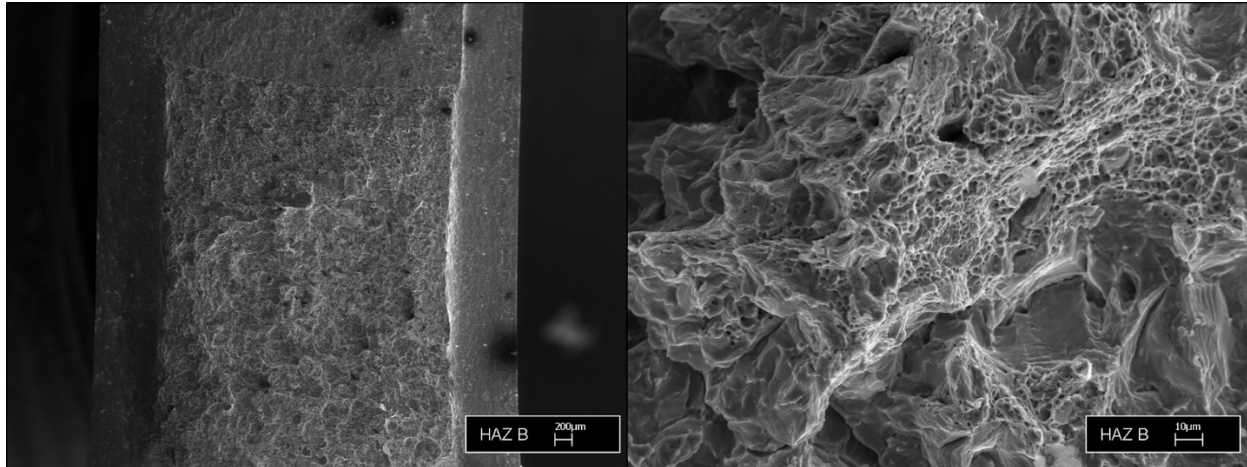
Figure 3-4. HAZ B material prototypical fractography images. Left shows a broad overview of the fracture surface, where the notches are the smooth edges, the fatigue pre-crack is visible as the smooth region at the top, and the crack grown in the test proceeds down the image. Right shows a higher magnification of the test crack region.
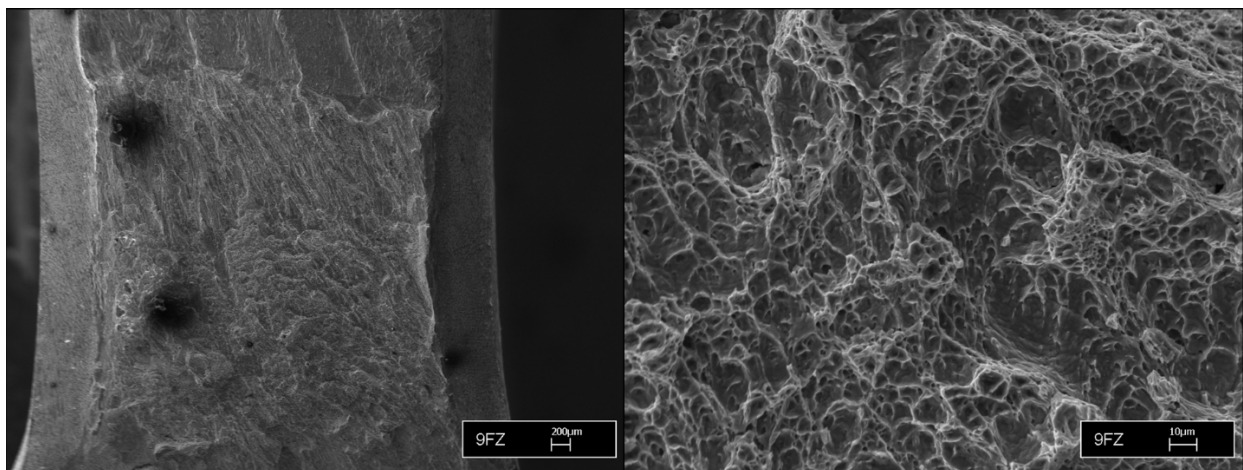
Figure 3-5. 9FZ material prototypical fractography images. Left shows a broad overview of the fracture surface, where the notches are the smooth edges, the fatigue pre-crack is visible as the smooth region at the top, and the crack grown in the test proceeds down the image. Right shows a higher magnification of the test crack region.

3.2 Continuing Studies in Tritium Effects

The two studies reported below, on forging process effects and the properties of long-aged tritium exposed steels, continue and confirm results and trends reported in previous years. In older forgings, 304L specimens display the same continuing reduction in fracture toughness reported in the 21-6-9 system. In these materials, toughness values decreased by over 95%. In more modern stem, cup, and block forgings of 316L and 304L materials an apparent plateau is observed in the latest round of testing after initial losses in fracture toughness of ~66%. Further testing in out years will elucidate whether this is a true plateau in embrittlement, or if it can be attributed to the variation and small sample sets inherent to this research program.

3.2.1 Forging process effects study

Additional fracture mechanics tests were conducted on specimens from a continuing project on types 316L and 304L forgings, charged in 2012[10]. Specimens tested had been aged for ~6.5 years. These tests represent an additional data point at higher (~1100 appm) helium contents. Analysis of these results is ongoing, and they will be reported in a later document. Qualitatively, in the tested samples, a seeming plateau is revealed in the recent tests at higher helium content, where toughness values are similar to the results previously reported at 650 appm He. A final aging of tritium exposed specimens from this study is planned to be tested in 2021 which will test if this is a true plateau, or merely a reduction in the rate of embrittlement.

3.3 Long-Aged Stainless Steels and Weldments

Additional testing has been completed on historical samples discussed in previous SRNL annual reports [8]. These results are added to the chart in Figure 3-6 which summarizes all the historical data to date from these studies. The oldest tested samples documented here were aged to build helium for over 16 years.
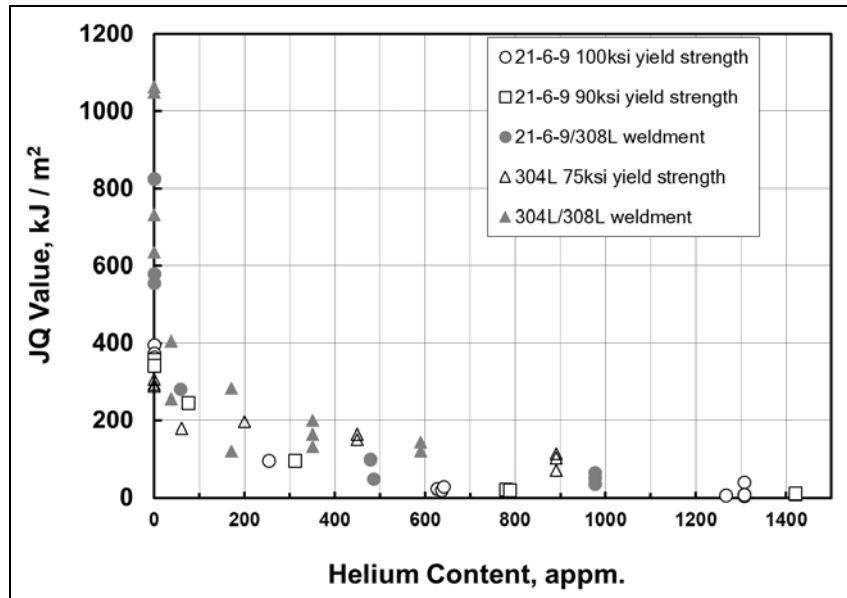
Figure 3-6. Reduction in Fracture Toughness with increasing helium content for types 304L and 21-6-9 stainless steel base metals and their weldments. New data shown in the 304L material above 500 appm helium. Reproduced from [19]

Table 3-3. Mechanical Properties and Fracture Toughness Values for a range of aging times with Tritium. Includes data previously reported in SRNL-STI-2018-00036[8]

Material Description	Mechanical Properties			Average Fracture Toughness Values				
	Ferrite	Yield Strength	Ultimate Strength	J_Q as-Received	J_Q Tritium-Charged & Aged 6 Mos.	J_Q Tritium-Charged & Aged 30 Mos.	J_Q Tritium-Charged & Aged 68 Mos.	J_Q Tritium-Charged & Aged 195 Mos.
Specimen ID	%	MPa	MPa	kJ/m^2	kJ/m^2	kJ/m^2	kJ/m^2	kJ/m^2
H94 - Forged Type 21-6-9	~0	685	960	370	245	96	24	7
F9 – Forged 21-6-9 low yield	~0	601	960	350	245	96	21	10
F97 - HERF Type 21-6-9	~0	723	961	211	121	70	29	7
F4 - Forged Type 304L	~0	462	724	296	179	195	158	95
48 - Normal Ferrite Weldment Type 304L/308L	8	427	607	870	330	202	165	132
98 - 21-6-9/308L	6	416	681	568	281	53	74	51
49 - High Ferrite Weldment Type 304L/309L	33	572	745	124	-	48	-	28

3.4 Small angle x-ray scattering

Small angle x-ray scattering (SAXS) measurements were conducted at the Advanced Photon Source (APS) at Argonne National Laboratory (ANL) facility on samples from SRNL. The goal of these tests was to determine if SAXS could be used to probe the size, spacing, and pressure distribution of helium bubbles derived from tritium decay in selected steel samples. The critical property in resolving these features is the scattering contrast, derived from the x-ray/electron-cloud interactions in the sample. This is analogous to previous experiments conducted at Oak Ridge National Laboratory with small angle neutron scattering (SANS) [8], where the scattering contrast for neutrons arises from interactions with nuclei. Because of the operational characteristics of the APS facility, including its very high brilliance, measurements can be conducted very quickly compared to similar SANS measurements. These data, combined with first principles calculations, shown together in Figure 3-7, have revealed that in the complex microstructures of interest to these aging studies, scattering from helium bubbles will be overwhelmed by scattering from the native microstructure. Specifically, the orange line is a plot of the predicted scattering from a hard sphere model of the helium bubbles, which can be seen to be overwhelmed by the scattering from the sample itself, in blue. Shown in dashed green is the same model with greatly increased contrast between matrix and bubble features to show the general shape of the predicted scattering, as a reference.
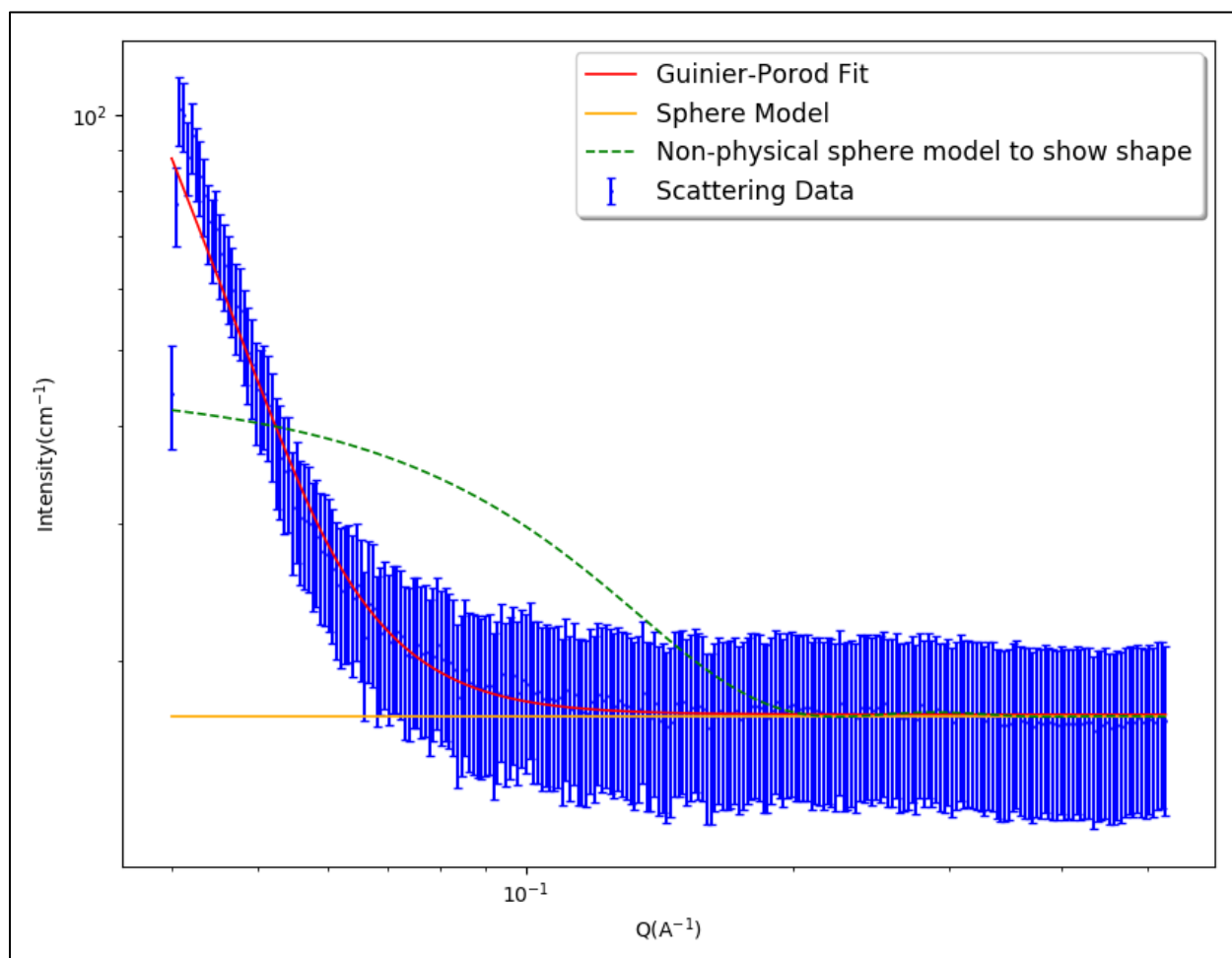
Figure 3-7. Data and models of scattering from a specimen cut from a 304L block forging. Data and error bars are shown in blue, and a shape independent Guinier-Porod fit of the data is shown as the red line. The dashed green line shows a hard sphere model with scattering contrast overemphasized to show the shape of the function, and the orange line shows the same model with physically realistic contrast

Studies in the literature using SAXS to examine helium bubble distributions have shown success, but only with model systems using pure material that reduce the problem of competing scattering centers[20]. This provides further rationale for why studies using SANS, while time consuming, are currently the best available option to gather statistically powerful bulk-averaged data on helium bubble microstructures in complex materials.

3.5 TDS

Samples from previous studies were sectioned, hermetically packaged, and shipped to SNL/NM for thermal desorption spectroscopy (TDS). Specifically, these were forged samples processed with HERF (High Energy Rate Forging) and screw press forging methods at 871 ºC, (see report SAND2017-5637C). Figure 3-8 shows preliminary results from TDS courtesy of C. S. Snow. These data will help identify the mechanisms and microstructural phenomena underlying tritium solubility and the formation of helium bubbles in structural materials.
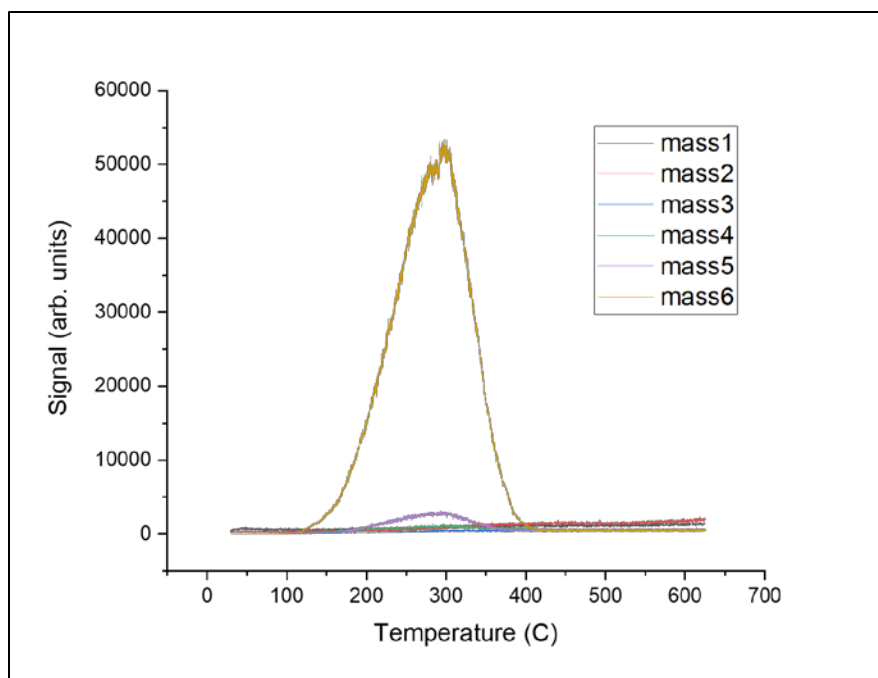
Figure 3-8. Thermal Desorption Spectroscopy results showing mass spectroscopy data of species released during heating of the appropriate sample. Peaks are associated with characteristic trap sites involved in the material-solute atom interaction (courtesy C.S. Snow, SNL/NM)

3.6 <u>PNNL FIB and SNL TEM progress</u>

 While the samples for TDS were sealed and shipped, sister samples were also packaged and shipped to PNNL for Focused Ion Beam (FIB) milling. Figure 3-9 left panel shows a specimen milled by B. W. Arey – PNNL. This specimen (lamella) was taken from a HERF 304L sample aged for 3 years after tritium charging. After milling specimens (lamella) were sent to SNL-CA for TEM examination. Importantly, the lamellae contain small enough quantities of tritium they can be handled in the clean TEM at SNL-CA. The right panel of Figure 3-9 shows a transmission microscopy image of a lamella, revealing helium bubbles, images courtesy D. L. Medlin – SNL
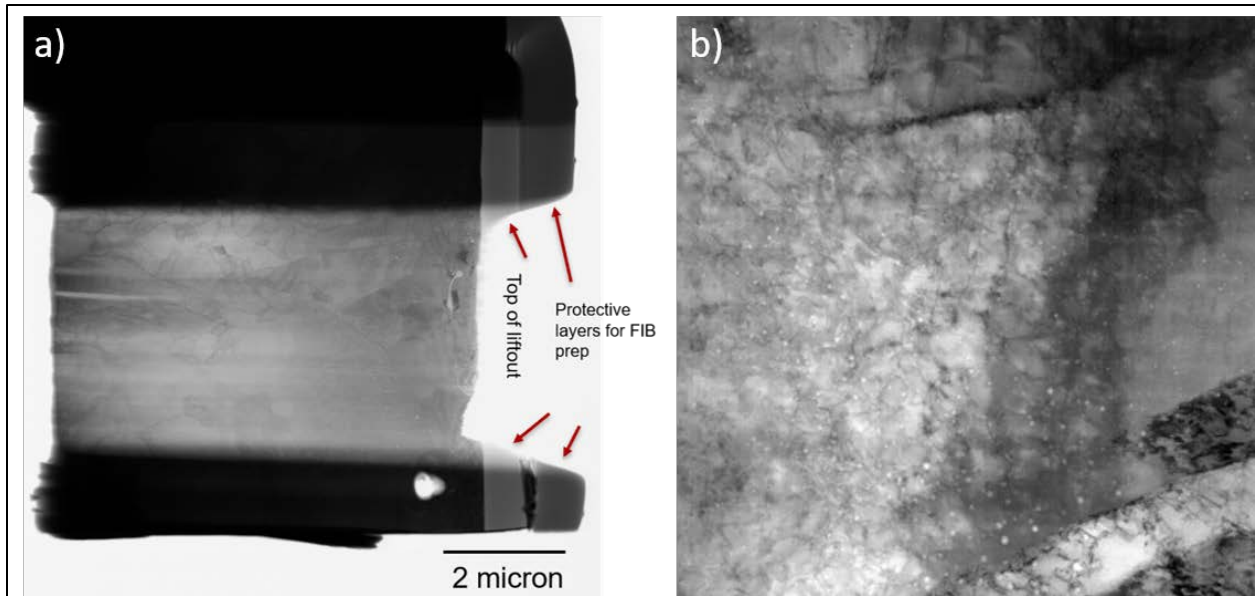
Figure 3-9. TEM results from showing a) a low magnification of the FIB prepared lamella and b) a higher magnification TEM micrograph from the same lamella revealing helium bubbles in the microstructure at high magnification (courtesy D. L. Medlin – SNL)

4.0 Progress with laboratory renovations and updates

Several renovations and updates have been made to the laboratory where mechanical testing on tritium exposed materials is conducted. The floor was removed and replaced as part of an asbestos abatement program, shown before and after in Figure 4-1.

Figure 4-1. Before (left) and After (right) replacement of flooring in mechanical testing lab

New equipment has also been installed and put into operation. An Instron E10000 load frame (Figure 4-2 left) brings the ability to conduct static and dynamic testing, including fatigue tests, at moderate loads. This machine will ease future increased workloads while providing expanded capability for dynamic testing in future studies. A new sample freezer (Figure 4-2 right) significantly increases the capacity for sample storage at -80°C, important for preventing the off gassing of tritium from pre-charged samples as they age.

Figure 4-2. Instron E10000 electric dynamic mechanical load frame (left) and new sample storage freezer (right).

5.0 Summary and Conclusions

- A new series of samples provided by SNL/CA was charged in July 2019. These samples comprise type 304L stainless steel material, smooth and notched tensile specimens, several strengths of tube tensile specimens in as-heat-treated and welded conditions, and smooth tensile specimens of type 316L stainless steel, provided by SNRL.

- The 1st of 4 different aging timepoints of tritium precharged FZ/HAZ type 304L and 21-6-9 weld specimens were tested. The magnitude of embrittlement with moderate helium and tritium levels is in agreement with historical data in similar materials. However, the FZ and HAZ results mark the first measurements of welds and HAZ that are relevant to the current stockpile. Longer aged samples will be tested in out years.

- The Stem, Cup, and Block forging study initiated in 2015[10] exhibited an average loss in toughness of 68% with 650 appm He. Longer aged samples tested this year with 1100 appm He exhibited similar losses in toughness suggesting a diminishing effect of the helium.

- Additional testing of a variety of long-aged samples has confirmed and extended previous trends, with measured losses in fracture toughness reaching as high as 98% in forged type 21-6-9 stainless steels with high initial yield strength aged for more than 16 years.

- Renovations to the mechanical testing lab and the procurement of new sample storage space at SRNL has been completed, to accommodate the planned increase in testing with joint projects from SRNL/SNL.

6.0 References

[1]   G. R. Caskey, "Hydrogen Effects in Stainless Steel," in *Hydrogen Degradation of Ferrous Alloys*, R. A. Oriani, J. P. Hirth, and M. A. Smialowski, Eds., ed Park Ridge, NJ: Noyes Publishing, 1985, pp. 822-862.

[2]   G. Caskey Jr, "Tritium-helium effects in metals," *Fusion Technology,* vol. 8, pp. 2293-2298, 1985.

[3]   S. L. Robinson and G. J. Thomas, "Accelerated Fracture due to Tritium and Helium in 21-6-9 Stainless Steel," *Metallurgical Transactions A,* vol. 22A, pp. 879-885, 1991.

[4]   S. L. Robinson, "The Effects of Tritium on the Flow and Fracture Stress of Austenitic Stainless Steels," in *Hydrogen Effects on Material Behavior*, N. R. Moody and A. W. Thompson, Eds., ed Warrendale PA: TMS, 1990, pp. 433-445.

[5]   S. Robinson and N. Moody, "The effect of hydrogen, tritium and decay helium on the fracture toughness of a stainless steel superalloy," *Journal of Nuclear Materials,* vol. 140, pp. 245-251, 1986.

[6]   "ASTM E1820-18a "Standard Test Method for Measurement of Fracture Toughness"," in *1999 Annual Book of ASTM Standards Volume 3.01: Metals-Mechanical Testing; Elevated and Low-Temperature Tests; Metallography;*, ed: American Society for Testing and Materials, 2018.

[7]   J. A. Ronevich, B. P. Somerday, C. W. San Marchi, and D. K. Balch, "Fracture threshold measurements of hydrogen precharged stainless steel weld fusion zones and heat affected zones," in *ASME 2015 Pressure Vessels and Piping Conference*, 2015.

[8]   M. J. Morgan, D. Hitchcock, T. Krentz, J. McNamara, and A. Duncan, "2017 Accomplishments–Tritium Aging Studies on Stainless Steel Weldments and Heat-Affected Zones," SRNL-STI-2018-00036 Savannah River Site (SRS), Aiken, SC (United States)2018.

[9]   T. M. Krentz, D. A. Hitchcock, M. J. Morgan, J. A. Ronevich, R. Sills, C. San Marchi*, et al.*, "Fracture Toughness Properties of Tritium-Charged-and-Aged Stainless Steels: SRNL and SNL Collaboration Test Plan and 2018 Results," SRNL-STI-2019-00022 Savannah River National Laboratory, Aiken, SC (United States)2019.

[10]   M. J. Morgan, "2015 Accomplishments - Tritium Aging Studies on Stainless Steel: Effects of Hydrogen Isotopes, Crack Orientation, and Specimen Geometry on Fracture Toughness," SRNL-STI-2016-00060 Savannah River National Laboratory, Aiken, SC2015.

[11]   C. San Marchi, B. P. Somerday, and S. L. Robinson, "Permeability, Solubility, and Diffusivity of Hydrogen Isotopes in Stainless Steels at High Gas Pressures," *International Journal of Hydrogen Energy,* vol. 32, pp. 100-116, 2007.

[12]   C. San Marchi and B. Somerday, "Technical reference on hydrogen compatibility of materials," Sandia National Laboratories SANDIA REPORT SAND2008-1163 2008.

[13]   J. A. Ronevich, C. San Marchi, and D. K. Balch, "Temperature Effects on Fracture Thresholds of Hydrogen Precharged Stainless Steel Welds," in *ASME 2017 Pressure Vessels and Piping Conference*, 2017, pp. V06BT06A040-V06BT06A040.

[14]   G. E. Dieter and D. J. Bacon, *Mechanical Metallurgy* vol. 3. New York: McGraw-Hill, 1986.

[15]   J. T. Busby, M. C. Hash, and G. S. Was, "The relationship between hardness and yield stress in irradiated austenitic and ferritic steels," *Journal of Nuclear Materials,* vol. 336, pp. 267-278, 2005.

[16]   ASTM, "A370 Standard Test Methods and Definitions for Mechanical Testing of Steel Products," ed: ASTM, 2019.

[17]   M. J. Morgan, S. L. West, and M. H. Tosten, "Effect of Tritium and Decay Helium on the Fracture Toughness Properties of Stainless Steel Weldments," in *Proceedings of the 8th Int. Conf. on Tritium Science and Technology,*, Rochester, NY, USA, 2008, pp. 501-505.

[18]   M. Morgan, "EFFECT OF HYDROGEN ISOTOPES ON THE FRACTURE TOUGHNESS PROPERTIES OF TYPES 316L AND 304L STAINLESS STEEL FORGINGS," *2019 ASME Pressure Vessels and Piping Division Conference,* 2019.

[19]   M. J. Morgan, D. A. Hitchcock, T. M. Krentz, and S. L. West, "Tritium Aging Effects on Fracture Toughness of Stainless Steel Weldments," *Fusion Science and Technology,* vol. 12th International Conference on Tritium Science and Technology, 2019 - accepted.

[20]   H. Rajainmäki, S. Linderoth, H. Hansen, R. Nieminen, and M. Bentzon, "Nucleation and growth of helium bubbles in aluminum between 20 and 900 K," *Physical Review B,* vol. 38, p. 1087, 1988.

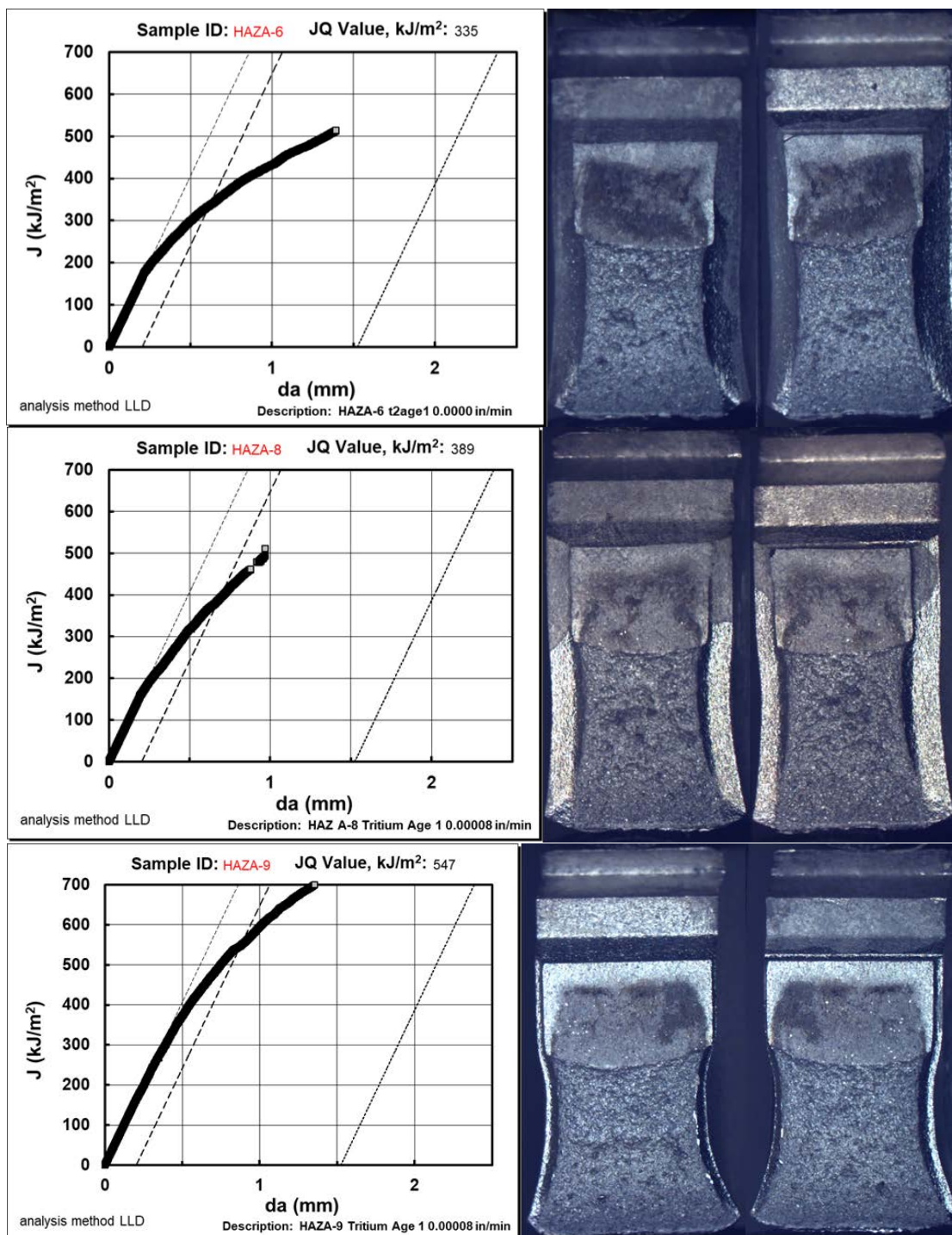**Appendix A. Compiled J-da curves and fracture surface images from weld bend bar testing**

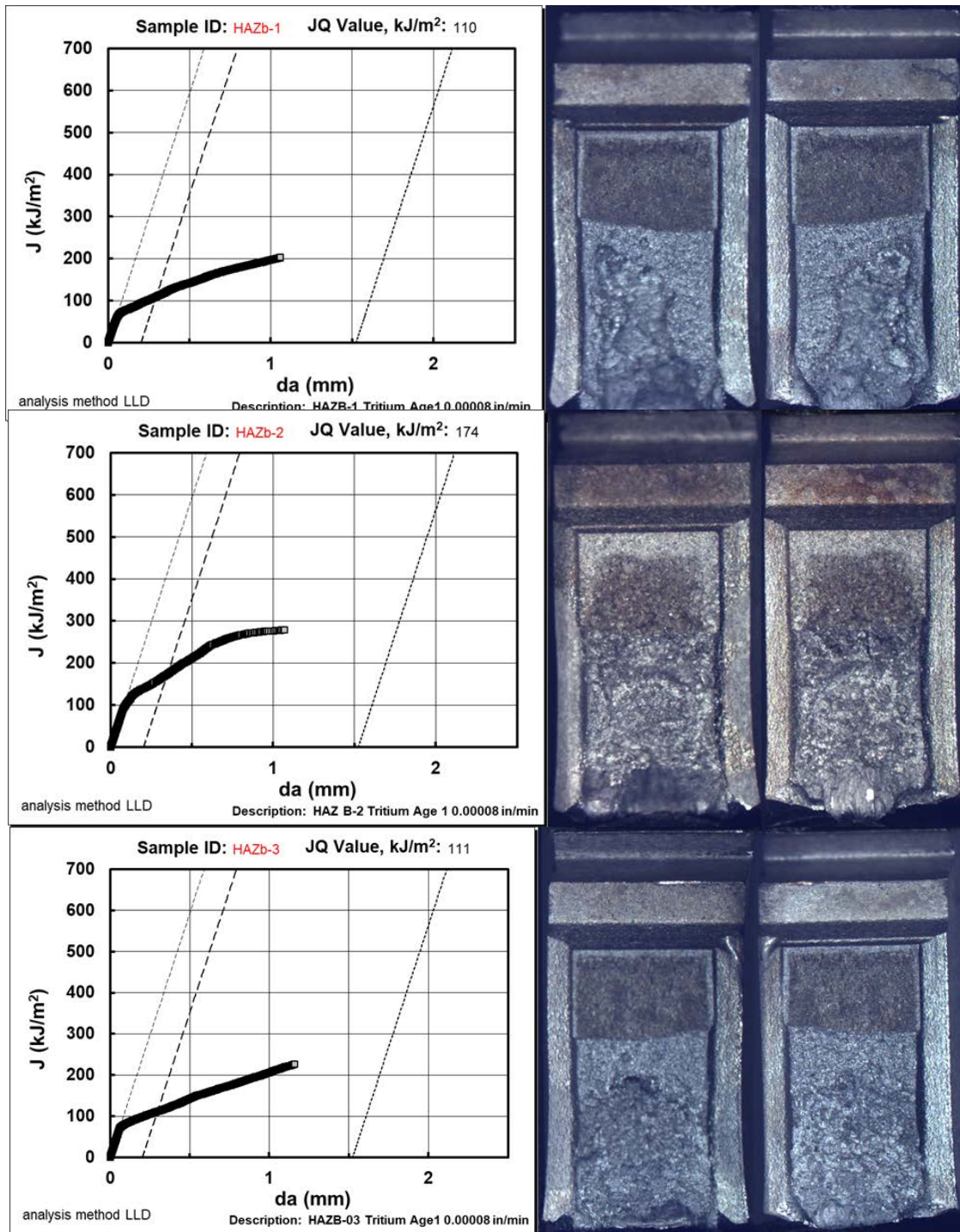**Figure 6-1. J vs. da crack growth resistance curves for 304L/308L weld HAZ**

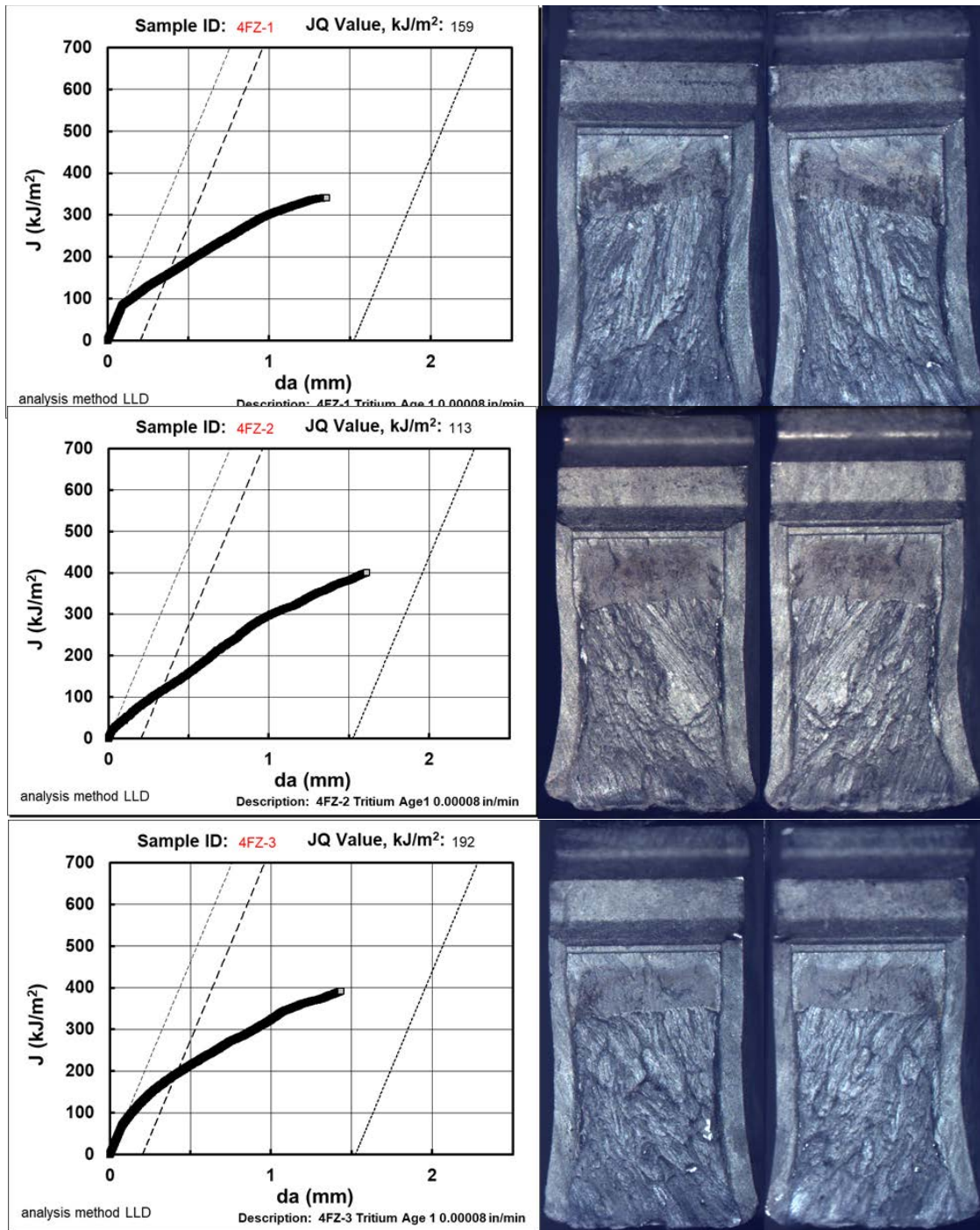**Figure 6-2. J vs. da crack growth resistance curves for 21-6-9/308L weld HAZ**

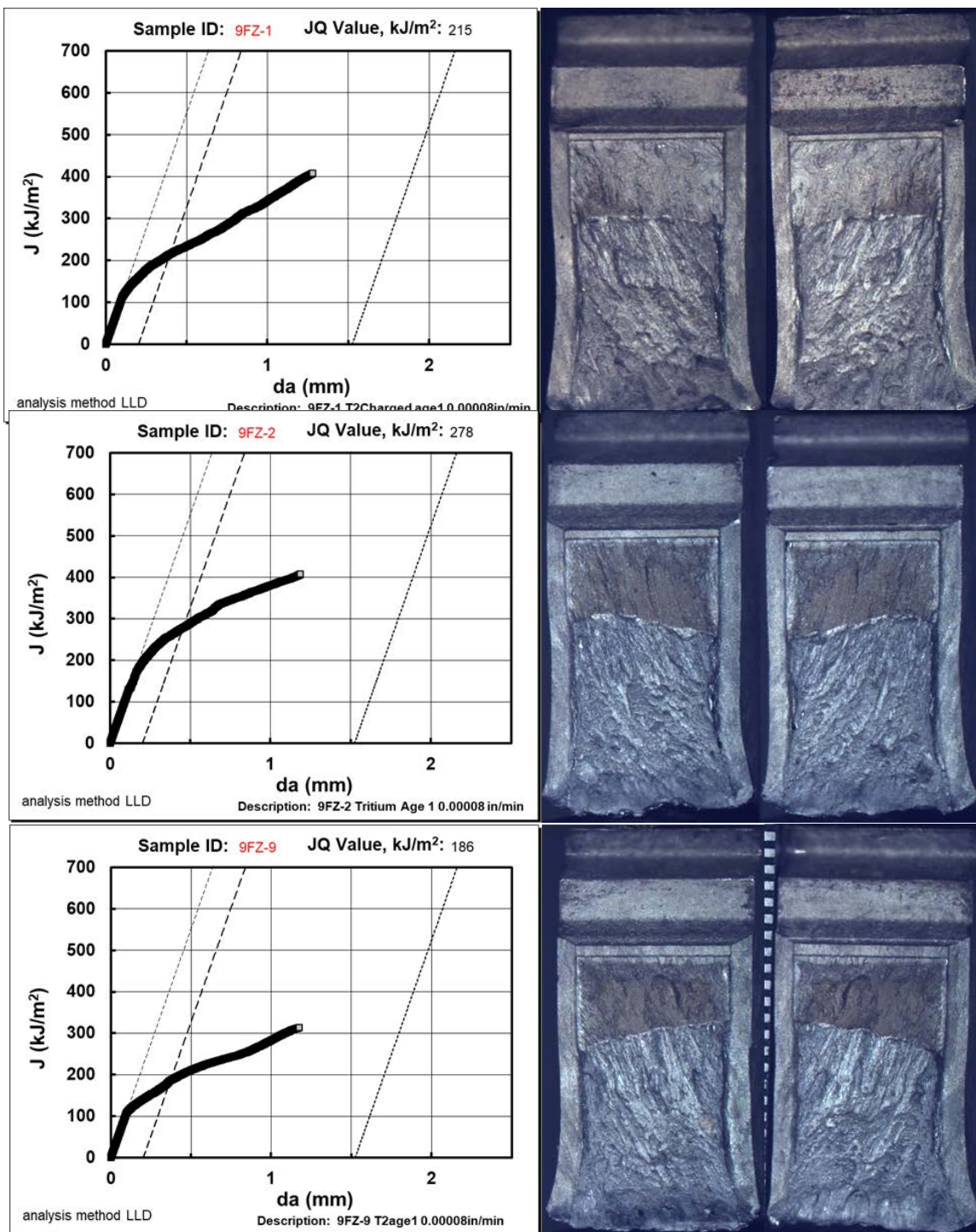**Figure 6-3. J vs. da crack growth resistance curves for 304L/308L weld FZ**

Figure 6-4. J vs. da crack growth resistance curves for 21-6-9/308L weld FZ